Proceedings of the ASME 2010 3rd Joint US-European Fluids Engineering Summer Meeting and 8th International Conference on Nanochannels, Microchannels, and Minichannels
FEDSM-ICNMM2010
August 1-5, 2010, Montreal, Canada

FEDSM-ICNMM2010-30654

RAPID AND SLOW DECOMPOSITION IN LARGE EDDY SIMULATION OF SCALAR TURBULENCE

L. Fang, L. Shao, J.P. Bertoglio
LMFA, École centrale de Lyon
69130, Ecully, BP 163, France
Université de Lyon, CNRS, INSA de Lyon
France

LP Lu
School of Jet Propulsion
Beihang University
100191 Beijing
China

ZS Zhang
Department of Engineering Mechanics
Tsinghua University
100084 Beijing
China

ABSTRACT

In large eddy simulation of turbulent flow, because of the spatial filter, inhomogeneity and anisotropy affect the subgrid stress via the mean flow gradient. A method of evaluating the mean effects is to split the subgrid stress tensor into "rapid" and "slow" parts. This decomposition was introduced by Shao *et al.* (1999) and applied to *A Priori* tests of existing subgrid models in the case of a turbulent mixing layer. In the present work, the decomposition is extended to the case of a passive scalar in inhomogeneous turbulence. The contributions of rapid and slow subgrid scalar flux, both in the equations of scalar variance and scalar flux, are analyzed. *A Priori* numerical tests are performed in a turbulent Couette flow with a mean scalar gradient. Results are then used to evaluate the performances of different popular subgrid scalar models. It is shown that existing models can not well simulate the slow part and need to be improved. In order to improve the modeling, an extension of the model proposed by Cui *et al.* (2004) is introduced for the slow part, whereas the Scale-Similarity model is used reproduce the rapid part. Combining both models, *A Priori* tests lead to a better performance. However, the remaining problem is that none eddy-diffusion model can correctly represent the strong scalar dissipation near the wall. This problem will be addressed in future work.

1 Introduction

Large-Eddy Simulation (LES) is a technique widely used in academic studies of turbulence, as well as applied to an increasing number of engineering projects. The LES approach consists in the simulation of the governing equations for the grid-scale (GS) motions with the introduction of models for the subgrid-scale (SGS) effects. The GS part of the field is obtained by introducing a spatial filter in order to remove the unresolvable, small scales of turbulence.

The problem of subgrid modeling in LES is complexified by the fact that different types of filters are used, generally depending on the flow to which the technique is applied. For example a spectral cut-off filter is often introduced in the case of homogeneous turbulence, whereas in most practical computations of inhomogeneous turbulence, filters in the physical domain are preferred. Furthermore Piomelli *et al.* [1] showed that the subgrid model formulation has to depend on the choice of the filter. Such as the scale-similarity model [2, 3], it is not suitable to use together with the spectral cut-off filter. A distinction has also to be made between LES with explicit filtering, and simulations where the filtering operation is implicit. Several subgrid models, such as the dynamic procedure introduced by Germano *et al.* [4] or the scale-similarity model, require an explicit filtering operation. With the necessity of physical-space filtering in inhomogeneous flows as well as the success and promise of subgrid models that require explicit filtering, it is clear that the role of filtering in SGS modeling deserves future attention.

The primary physical effect that requires modeling in LES is the net energy transfer between GS and SGS turbulent scales, which includes both the dominant dissipative effect associated with the forward transfer from large to small scales and the backward transfer from small to large scales. The backward transfer is often small compared to the forward transfer, but it can be dominant near a wall [5]. The theoretical background for modeling the effect of small scales in LES has essentially remained within the framework of homogeneous turbulence. Various theories of SGS modeling have been developed by Kraichnan [6], Leslie and Quarini [7], Leith [8], Chollet and Lesieur [9], Bertoglio and Mathieu [10, 11], and recently L. Marstorp [12], etc. In most cases the Kolmogorov theory for the energy cascade is implicitly used to represent the SGS transfer. However, it is unlikely that, for routine engineering applications, computational resources will allow the fine resolution required for the approximation of isotropy and homogeneity of the small-scale turbulence to be acceptable. For the important applications where the turbulence is inhomogeneous, fundamental studies are rare. Schumann [13] introduced a two-part eddy viscosity model: a *homogeneous* part that accounts for the "locally isotropic" part of the SGS stress and an *inhomogeneous* part to represent the anisotropy associated with the use of a large filter size. The inhomogeneous part is directly related to the Reynolds-averaged strain rate in the spirit of a classical eddy viscosity closure. In spectral space, Laporta and Bertoglio [14] introduce a two-point closure for inhomogeneous turbulence. O'Neil and Meneveau [15] performed an experimental study of the SGS stress in an inhomogeneous turbulent wake. They found that the large coherent structures in the wake strongly affect the SGS stress. Therefore, the local inhomogeneity of the flow and the associated coherent structures influences the SGS stress in the wake and may require modeling. Shao *et al.* [16] introduced a "rapid-slow" decomposition of the subgrid terms in inhomogeneous turbulence, and studied the relationship between the mean flow and subgrid stress in a turbulent mixing layer. The aim of the present work is to extend this decomposition to the case of a passive scalar turbulence.

The understanding of small-scale fluctuations in scalar fields, such as temperature, pollutant density, chemical or biological species concentration, advected by turbulent flow is of great interest in both theoretical and practical domains [17, 18]. In the presence of mean scalar gradients, the passive scalar field becomes anisotropic, which introduces its particular behavior with respect to small-scale anisotropy [19, 20], structures [21] and turbulent scalar fluxes [22, 23]. Adding velocity shear to the problem, complexifies the problem more, introducing non trivially scaling turbulent fluxes in both the cross-stream and stream-wise direction [24]. The case of simultaneous shear and scalar gradient was studied by LES in [25]. Attempts to use LES for the study of scalar mixing in complex flows (including solid boundaries, shear and scalar gradients) [26–30] show that each subgrid model has its limitation in predicting the GS scalar mixing. Particularly, in wall-bounded turbulence, the near-wall energy backscatter (of both energy and scalar variance) can not be represented well, since the influence of the mean gradients is not considered. On the contrary, in the Cui Model, the subgrid scalar flux is explicitly related to the mean shear and mean scalar gradient [31]. However, the "rapid" part still can not be modeled, since it strongly depends on the properties of the filter.

In the present study the implications of physical-space filtering in SGS modeling of incompressible inhomogeneous scalar turbulence is investigated. The rapid-slow decomposition is introduced to represent the interactions between GS and SGS motions. We explore the various consequences of LES of inhomogeneous scalar turbulence on the filtering approach, on the energetics of the interaction between grid scales and subgrid scales, on the anisotropy of this interaction, on the contributions in the equations of scalar flux, and, finally on the fidelity of existing SGS models.

2 Basic equations of inhomogeneous anisotropic scalar turbulence

In order to show the exact interactions between velocity and scalar in subgrid transfer, it is necessary to derive the basic equations of inhomogeneous anisotropic scalar turbulence. Before derivation, we would like to introduce two important concepts in this paper. The first one is the filter operator in LES. A filter operator divides any variable ϕ into two parts $\phi = \phi^< + \phi^>$, in which $\phi^<$ is the GS part and $\phi^>$ is the SGS part. A filter in physical space can be represented by introducing a filter kernel $\int G(\boldsymbol{x}-\boldsymbol{x}')d\boldsymbol{x}' = 1$, and the GS part ($\phi^<$) can be denoted as $\phi^<(\boldsymbol{x}) = \int G(\boldsymbol{x}-\boldsymbol{x}')\phi(\boldsymbol{x}')d\boldsymbol{x}'$.

In general, the filter operator has the following properties:

$$(\phi+\psi)^< = \phi^< + \psi^<, \qquad \left(\frac{\partial\phi}{\partial t}\right)^< = \frac{\partial\phi^<}{\partial t}. \tag{1}$$

Besides, $\phi^{<<} \neq \phi^<, (\phi^<)^> \neq 0$ when filtering is performed with a physical space filter, which is applied in this paper. The commutability between filtering and spatial derivation will be discussed later.

By contraries, the second concept is the ensemble average operator, which is a statistical operation. Every physical variable ϕ can be divided into mean and fluctuating part $\phi = \langle\phi\rangle + \phi'$, in which the symbol $\langle\rangle$ is the arithmetic mean from experiments.

Comparing with the filter operator, the ensemble average has different properties:

$$\begin{aligned} &\langle\phi+\psi\rangle = \langle\phi\rangle + \langle\psi\rangle, \qquad \left\langle\frac{\partial\phi}{\partial s}\right\rangle = \frac{\partial\langle\phi\rangle}{\partial s}, s = \boldsymbol{x}, t \\ &\langle\langle\phi\rangle\rangle = \langle\phi\rangle, \qquad \langle\phi'\rangle = 0. \end{aligned} \tag{2}$$

For the ensemble average operator, the following commutations can be obtained because of linear property:

$$\langle\phi\rangle^{<}=\langle\phi^{<}\rangle,\left\langle\frac{\partial\phi}{\partial x_i}\right\rangle=\frac{\partial\langle\phi\rangle}{\partial x_i}. \tag{3}$$

However, filtering and differentiation do not commute when the filter width is nonuniform in space [32]. A general class of commutative filters was introduced by Vasilyev [33] and Marsden [34] to decrease the commutation error in LES equations for inhomogeneous filter width. In order to avoid this difficulty, in this paper we always use homogeneous meshes in *A Priori* tests, so that the filtering and differentiation could commute, *i.e.* $\left(\frac{\partial\phi}{\partial x_i}\right)^{<}=\frac{\partial\phi^{<}}{\partial x_i}$.

Based on the concepts of filter and ensemble average, we will write the governing equations of scalar variance and scalar flux in the following part, respectively.

2.1 Governing equations of scalar variance

For a passive scalar θ, the governing equation is

$$\frac{\partial\theta}{\partial t}+u_j\frac{\partial\theta}{\partial x_j}=\kappa\frac{\partial^2\theta}{\partial x_j\partial x_j}, \tag{4}$$

where κ is diffusion coefficient. Taking ensemble average, it becomes

$$\frac{\partial\langle\theta\rangle}{\partial t}+\langle u_j\rangle\frac{\partial\langle\theta\rangle}{\partial x_j}=\kappa\frac{\partial^2\langle\theta\rangle}{\partial x_j\partial x_j}-\frac{\partial}{\partial x_j}\langle u_j'\theta'\rangle. \tag{5}$$

Multiplying Eq. (5) by $2\langle\theta\rangle$ leads to the equation for mean scalar variance

$$\begin{aligned}\frac{\partial\langle\theta\rangle^2}{\partial t}+\langle u_j\rangle\frac{\partial\langle\theta\rangle^2}{\partial x_j}=&2\kappa\langle\theta\rangle\frac{\partial^2\langle\theta\rangle}{\partial x_j\partial x_j}+2\left\langle u_j'\theta'\right\rangle\frac{\partial\langle\theta\rangle}{\partial x_j}\\&-2\frac{\partial}{\partial x_j}\left(\langle\theta\rangle\langle u_j'\theta'\rangle\right).\end{aligned} \tag{6}$$

Now we consider the scalar transport in LES. The governing equation for the resolved scalar can be written as

$$\frac{\partial\theta^{<}}{\partial t}+u_j^{<}\frac{\partial\theta^{<}}{\partial x_j}=\kappa\frac{\partial^2\theta^{<}}{\partial x_j\partial x_j}-\frac{\partial\tau_{\theta j}}{\partial x_j}, \tag{7}$$

where $\tau_{\theta j}$ is the subgrid-scale scalar flux defined as $\tau_{\theta j}=(u_j\theta)^{<}-u_j^{<}\theta^{<}$.

The governing equation for resolved mean scalar variance is

$$\begin{aligned}&\frac{1}{2}\frac{\partial\langle\theta^{<}\rangle^2}{\partial t}+\frac{1}{2}\langle u_j^{<}\rangle\frac{\partial\langle\theta^{<}\rangle^2}{\partial x_j}\\=&\kappa\langle\theta^{<}\rangle\frac{\partial\langle\theta^{<}\rangle}{\partial x_j\partial x_j}-\frac{\partial}{\partial x_j}\left(\langle\tau_{\theta j}\rangle\langle\theta^{<}\rangle-\left\langle u_j'^{<}\theta'^{<}\right\rangle\langle\theta^{<}\rangle\right)\\&+\left\langle u_j'^{<}\theta'^{<}\right\rangle\frac{\partial\langle\theta^{<}\rangle}{\partial x_j}+\langle\tau_{\theta j}\rangle\frac{\partial\langle\theta^{<}\rangle}{\partial x_j},\end{aligned} \tag{8}$$

while the transport of resolved scalar fluctuation is

$$\begin{aligned}&\frac{1}{2}\frac{\partial\langle\theta'^{<2}\rangle}{\partial t}+\frac{1}{2}\langle u_j^{<}\rangle\frac{\partial\langle\theta'^{<2}\rangle}{\partial x_j}\\=&\kappa\left\langle\theta'^{<}\frac{\partial\theta'^{<}}{\partial x_j\partial x_j}\right\rangle-\frac{\partial}{\partial x_j}\left(\left\langle\tau_{\theta j}'\theta'^{<}\right\rangle-\left\langle u_j'\theta'\theta'\right\rangle\right)\\&-\langle u_j'^{<}\theta'^{<}\rangle\frac{\partial\langle\theta^{<}\rangle}{\partial x_j}+\left\langle u_j'^{<}\theta'^{<}\frac{\partial\theta'^{<}}{\partial x_j}\right\rangle+\left\langle\tau_{\theta j}'\frac{\partial\theta'^{<}}{\partial x_j}\right\rangle.\end{aligned} \tag{9}$$

In the right hand sides of Eqs. (8) and (9), $\left\langle u_j'^{<}\theta'^{<}\right\rangle\frac{\partial\langle\theta^{<}\rangle}{\partial x_j}$ is an exchange term between mean and fluctuating scalar variances. The term $\left\langle u_j'^{<}\theta'^{<}\frac{\partial\theta'^{<}}{\partial x_j}\right\rangle$ in Eq. (9) represents the self-interaction between the velocity and scalar fluctuations. The terms $\langle\tau_{\theta j}\rangle\frac{\partial\langle\theta^{<}\rangle}{\partial x_j}$ and $\left\langle\tau_{\theta j}'\frac{\partial\theta'^{<}}{\partial x_j}\right\rangle$ are focused on, since they denote the interactions between the SGS scalar flux $\tau_{\theta j}$ and the GS scalar gradient $\frac{\partial\theta^{<}}{\partial x_j}$. Further discussion on these terms is presented in Sec. 3. Other terms in Eqs. (8) and (9) represent scalar dissipation, diffusion and turbulent convection.

2.2 Governing equations of scalar flux

In order to write the governing equation for scalar flux $u_i\theta$, we start from the Navier-Stokes equation for incompressible turbulence

$$\frac{\partial u_i}{\partial t}+u_j\frac{\partial u_i}{\partial x_j}=-\frac{1}{\rho}\frac{\partial p}{\partial x_i}+\nu\frac{\partial^2u_i}{\partial x_j\partial x_j}, \tag{10}$$

where ν is the kinematic viscosity. Taking ensemble average, the equation can be written as

$$\frac{\partial\langle u_i\rangle}{\partial t}+\langle u_j\rangle\frac{\partial\langle u_i\rangle}{\partial x_j}=-\frac{1}{\rho}\frac{\partial\langle p\rangle}{\partial x_i}+\nu\frac{\partial^2\langle u_i\rangle}{\partial x_j\partial x_j}-\frac{\partial}{\partial x_j}\langle u_j'u_i'\rangle, \tag{11}$$

and the governing equation of velocity fluctuation is

$$\frac{\partial u_i'}{\partial t}+\langle u_j\rangle\frac{\partial u_i'}{\partial x_j}+u_j'\frac{\partial\langle u_i\rangle}{\partial x_j}=-\frac{1}{\rho}\frac{\partial p'}{\partial x_i}+\nu\frac{\partial^2 u_i'}{\partial x_j\partial x_j} -\frac{\partial}{\partial x_j}\left(u_i'u_j'-\langle u_i'u_j'\rangle\right). \tag{12}$$

In LES, with the definition of subgrid stress tensor $\tau_{ij}=(u_iu_j)^<-u_i^<u_j^<$, the governing equation is

$$\frac{\partial u_i^<}{\partial t}+u_j^<\frac{\partial u_i^<}{\partial x_j}=-\frac{1}{\rho}\frac{\partial p^<}{\partial x_i}+\nu\frac{\partial^2 u_i^<}{\partial x_j\partial x_j}-\frac{\partial\tau_{ij}}{\partial x_j}. \tag{13}$$

The filtered mean equation reads

$$\frac{\partial\langle u_i^<\rangle}{\partial t}+\langle u_j^<\rangle\frac{\partial\langle u_i^<\rangle}{\partial x_j}=-\frac{1}{\rho}\frac{\partial\langle p^<\rangle}{\partial x_i}+\nu\frac{\partial^2\langle u_i^<\rangle}{\partial x_j\partial x_j} -\frac{\partial\langle\tau_{ij}\rangle}{\partial x_j}-\frac{\partial}{\partial x_j}\langle u_i'^<u_j'^<\rangle. \tag{14}$$

Thus the governing equation for resolved mean scalar flux is

$$\begin{aligned}\frac{\partial\langle u_i^<\rangle\langle\theta^<\rangle}{\partial t}+\langle u_j^<\rangle\frac{\partial\langle u_i^<\rangle\langle\theta^<\rangle}{\partial x_j}&=\nu\langle\theta^<\rangle\frac{\partial^2\langle u_i^<\rangle}{\partial x_j\partial x_j}+\kappa\langle u_i^<\rangle\frac{\partial^2\langle\theta^<\rangle}{\partial x_j\partial x_j}\\ &-\frac{\partial}{\partial x_i}\left[\frac{1}{\rho}\left(\langle\theta^<\rangle\langle p^<\rangle\right)+\langle\theta^<\rangle\langle\tau_{ij}\rangle\right.\\ &\left.+\langle u_i^<\rangle\langle\tau_{\theta j}\rangle+\langle u_i'^<u_j'^<\rangle\langle\theta^<\rangle+\langle u_j'^<\theta'^<\rangle\langle u_i^<\rangle\right]\\ &+\frac{1}{\rho}\langle p^<\rangle\frac{\partial\langle\theta^<\rangle}{\partial x_j}+\langle u_i'^<u_j'^<\rangle\frac{\partial\langle\theta^<\rangle}{\partial x_j}+\langle u_j'^<\theta'^<\rangle\frac{\partial\langle u_i^<\rangle}{\partial x_j}\\ &+\langle\tau_{ij}\rangle\frac{\partial\langle\theta^<\rangle}{\partial x_j}+\langle\tau_{\theta j}\rangle\frac{\partial\langle u_i^<\rangle}{\partial x_j}\end{aligned} \tag{15}$$

and the governing equation for resolved fluctuating scalar flux is

$$\begin{aligned}\frac{\partial\langle u_i'^<\theta'^<\rangle}{\partial t}+\langle u_j^<\rangle\frac{\partial\langle u_i'^<\theta'^<\rangle}{\partial x_j}&=\kappa\left\langle u_i'^<\frac{\partial^2\theta'^<}{\partial x_j\partial x_j}\right\rangle+\nu\left\langle\theta'^<\frac{\partial^2 u_i'^<}{\partial x_j\partial x_j}\right\rangle\\ &-\frac{\partial}{\partial x_j}\left(\frac{1}{\rho}\langle\theta'^<p'^<\rangle+\langle\tau_{\theta j}'u_i'^<\rangle+\langle\tau_{ij}'\theta'^<\rangle+\langle u_i'^<u_j'^<\theta'^<\rangle\right)\\ &+\frac{1}{\rho}\left\langle p'^<\frac{\partial\theta'^<}{\partial x_i}\right\rangle-\langle u_i'^<u_j'^<\rangle\frac{\partial\langle\theta^<\rangle}{\partial x_j}\\ &-\langle u_j'^<\theta'^<\rangle\frac{\partial\langle u_i^<\rangle}{\partial x_j}+\left\langle(u_i'^<\theta'^<)\frac{\partial u_j'^<}{\partial x_j}\right\rangle\\ &+\left\langle\tau_{\theta j}'\frac{\partial u_i'^<}{\partial x_j}\right\rangle+\left\langle\tau_{ij}'\frac{\partial\theta'^<}{\partial x_j}\right\rangle.\end{aligned} \tag{16}$$

In Eqs. (15) and (16), we pay attention to the interaction between the subgrid stress and the scalar gradient, as well as the interaction between the subgrid scalar flux and the velocity gradient. The detailed analysis will be presented in Sec. 4.3.

3 Rapid-slow decomposition of subgrid scalar flux

Shao *et al.* [16] introduced a "rapid-slow" decomposition for subgrid stress. The SGS tensor τ_{ij} was split into two parts: a rapid part that explicitly depends on mean flow and a remaining slow part. The term "rapid" was used by analogy to the terminology introduced by Rotta [35] and Lumley [36] in the context of Reynolds-averaged modeling, where the component of the "pressure-strain" term that explicitly depends on the mean velocity gradient is referred to as the rapid part and the remainder as the slow part. Shao first extended this decomposition to LES, and applied it to the analysis of a turbulent mixing layer. The performance of classical Smagorinsky model and of scale-similarity model were then evaluated. However, subgrid scalar transport has not been analyzed yet. In this paper we propose the similar decomposition for subgrid scalar flux, which will be applied in the following analysis.

Similar to the decomposition of velocity field, the subgrid scalar flux $\tau_{\theta j}$ can be split into rapid and slow parts:

$$\tau_{\theta j}=\tau_{\theta j}^{rapid}+\tau_{\theta j}^{slow}, \tag{17}$$

in which

$$\begin{aligned}\tau_{\theta j}^{rapid}&=(\langle u_j\rangle\langle\theta\rangle)^<-\langle u_j\rangle^<\langle\theta\rangle^<\\ &\quad+(\langle u_j\rangle\theta')^<-\langle u_j\rangle^<\theta'^<+(u_j'\langle\theta\rangle)^<-u_j'^<\langle\theta\rangle^<\\ \tau_{\theta j}^{slow}&=(u_j'\theta')^<-u_j'^<\theta'^<.\end{aligned} \tag{18}$$

The rapid part corresponds to the interaction involving mean velocity or mean scalar; the slow part is the interaction between fluctuations.

In order to describe the effect of rapid and slow components of the SGS scalar flux in the transport process of scalar variance, the rapid and slow parts are further decomposed as:

$$\tau_{\theta j}^{rapid}=\langle\tau_{\theta j}^{rapid}\rangle+\tau_{\theta j}'^{rapid},\qquad \tau_{\theta j}^{slow}=\langle\tau_{\theta j}^{slow}\rangle+\tau_{\theta j}'^{slow} \tag{19}$$

It is clear that the mean rapid part is given by

$$\langle\tau_{\theta j}^{rapid}\rangle=(\langle u_j\rangle\langle\theta\rangle)^<-\langle u_j\rangle^<\langle\theta\rangle^<, \tag{20}$$

while the fluctuating rapid part is

$$\tau_{\theta j}'^{rapid}=(\langle u_j\rangle\theta')^<-\langle u_j\rangle^<\theta'^<+(u_j'\langle\theta\rangle)^<-u_j'^<\langle\theta\rangle^< \tag{21}$$

Similarly, the mean slow part is

$$\langle \tau_{\theta j}^{slow} \rangle = \langle (u_j' \theta')^{<} - u_j'^{<} \theta'^{<} \rangle \tag{22}$$

and the fluctuating slow part is

$$\tau_{\theta j}'^{slow} = \tau_{\theta j}^{slow} - \langle \tau_{\theta j}^{slow} \rangle \tag{23}$$

From these definitions above, we can also divide the terms of subgrid transport, which are shown in Sec. 2.1, into rapid and slow parts. For example in the governing equation of mean GS scalar variance (8), the second term in the right hand side is an interaction between the mean SGS scalar flux and mean GS velocity gradient. This term can be rewritten as

$$\langle \tau_{\theta j} \rangle \frac{\partial \langle \theta^{<} \rangle}{\partial x_j} = \langle \tau_{\theta j}^{rapid} \rangle \frac{\partial \langle \theta^{<} \rangle}{\partial x_j} + \langle \tau_{\theta j}^{slow} \rangle \frac{\partial \langle \theta^{<} \rangle}{\partial x_j}, \tag{24}$$

to isolate the effect of the rapid term. The slow term in Eq. (24) corresponds to the term identified by Jiménez *et al.* [37] as the SGS dissipation term. In the governing equation of GS scalar variance fluctuation (9), the same decomposition yields

$$\left\langle \tau_{\theta j}' \frac{\partial \theta'^{<}}{\partial x_j} \right\rangle = \left\langle \tau_{\theta j}'^{rapid} \frac{\partial \theta'^{<}}{\partial x_j} \right\rangle + \left\langle \tau_{\theta j}'^{slow} \frac{\partial \theta'^{<}}{\partial x_j} \right\rangle. \tag{25}$$

In inhomogeneous scalar turbulence, the rapid subgrid scalar flux strongly depends on the type of filter we use. In order to clarify the effect of the rapid part, we evaluate the magnitude of the mean rapid SGS scalar flux in the following part.

3.1 Magnitude of the mean rapid subgrid scalar flux

In channel turbulence, the rapid part is produced by the filter in normal direction, which is the only inhomogeneous direction. In order to study the properties of filters, we can define a 1-D filter operation in normal direction:

$$\varphi(y)^{<} = \frac{1}{\Delta(y)} \int_a^b G\left(\frac{y'-y}{\Delta(y)}, y \right) \varphi(y') dy' \tag{26}$$

where $\Delta(y)$ is filter width and $G(\eta, y)$ is the location-dependent filter function. Let $\eta = \dfrac{y-y'}{\Delta(y)}$, Eq. (26) can be written as

$$\varphi(y)^{<} = \int_{\frac{y-b}{\Delta(y)}}^{\frac{y-a}{\Delta(y)}} G(\eta, y) \varphi(y - \Delta(y)\eta) d\eta \tag{27}$$

Following the same processes of Marsden [34] and Vasilyev [33], taking the Taylor series expansion of $\varphi(y - \Delta(x)\eta)$ in powers of Δ, we could obtain

$$\varphi(y)^{<} = \varphi(y) + \sum_{l=n}^{\infty} \frac{(-1)^l}{l!} \Delta^l(y) M^l(y) \mathscr{D}_y^l \varphi(y) \tag{28}$$

where $M^l(y) = \int_{\frac{y-b}{\Delta(y)}}^{\frac{y-a}{\Delta(y)}} \eta^l G(\eta, y) d\eta = \begin{cases} 1, \, l = 0 \\ 0, \, l = 1, ..., n-1 \end{cases}$, $\mathscr{D}_y^l = \frac{d^l}{dy^l}$, in which n could represent a property of the filter. Thus the terms of subgrid scalar flux are expressed as

$$\begin{aligned}
&\langle \theta \rangle(y)^{<} \langle u_i \rangle(y)^{<} = \langle \theta \rangle(y) \langle u_i \rangle(y) \\
&+ \sum_{l=n}^{\infty} \frac{(-1)^l}{l!} \Delta^l(y) M^l(y) \left(\langle \theta \rangle(y) \mathscr{D}_y^l \langle u_i \rangle(y) + u_i(y) \mathscr{D}_y^l \langle \theta \rangle(y) \right) \\
&+ \sum_{l=n}^{\infty} \sum_{r=n}^{\infty} \frac{(-1)^{l+r}}{l!r!} \Delta^{l+r}(y) M^l(y) M^r(y) \mathscr{D}_y^l \langle \theta \rangle(y) \mathscr{D}_y^r \langle u_i \rangle(y) \\
&(\langle \theta \rangle(y) \langle u_i \rangle(y))^{<} = \langle \theta \rangle(y) \langle u_i \rangle(y) \\
&+ \sum_{l=n}^{\infty} \frac{(-1)^l}{l!} \Delta^l(y) M^l(y) \sum_{k=0}^{l} C_l^k \mathscr{D}_y^{l-k} \langle \theta \rangle(y) \mathscr{D}_y^k \langle u_i \rangle(y)
\end{aligned} \tag{29}$$

and the magnitude of the mean rapid part of subgrid scalar flux can be evaluated as:

$$\langle \theta \rangle(y)^{<} \langle u_i \rangle(y)^{<} - (\langle \theta \rangle(y) \langle u_i \rangle(y))^{<} = \begin{cases} O(\Delta^n(y)), \, n > 1 \\ O(\Delta^2(y)), \, n = 1 \end{cases} \tag{30}$$

In this chapter, we employ the homogeneous top-hat filter in physical space, which has $n = 1$, and

$$\langle \theta \rangle(y)^{<} \langle u_i \rangle(y)^{<} - (\langle \theta \rangle(y) \langle u_i \rangle(y))^{<} \propto \frac{\partial \langle \theta \rangle}{\partial y} \frac{\partial \langle u_i \rangle}{\partial y} \Delta^2(y) \tag{31}$$

It means that the mean rapid term is of Δ^2 magnitude. It will also be further verified by numerical simulation in the next section.

Marsden has also introduced the analysis on the 3-D filters when all three directions are inhomogeneous, and obtained the same conclusion [34]. However in this paper the streamwise and spanwise directions are both homogeneous, so we should only consider the inhomogeneous effects in normal direction, and a 1-D filter analysis is appropriate.

4 A Priori rapid-slow decomposition in Couette flow

A DNS case of Couette flow is used in evaluating the rapid and slow parts of scalar transport. The grids number

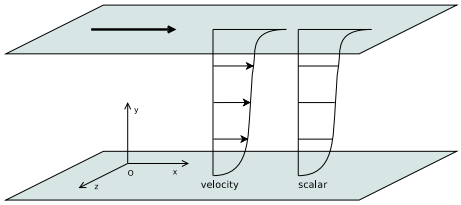

FIGURE 1. Sketch of computational domain, velocity profile and scalar profile.

is $192 \times 384 \times 96$ in streamwise, normal and spanwise directions respectively, and the corresponding computation domain is $4\pi H \times 2H \times 2\pi H$. Pseudo-spectral method is employed in calculation. The numerical details can be found from Xu *et al.* [38]. The Reynolds number is $\mathrm{Re}_H = 3200$ based on the bulk velocity U_m and the half width of the channel H, which is equivalent to a Reynolds number of 12800 in Kawamura's DNS results [26]. The scalar value is fixed to be 1 in the upper plane and 0 in the lower plane (in the following, the normal coordinate is related to the lower plane because of symmetry.). The molecular Prandtl number is $\mathrm{Pr} = 0.7$. The sketch of computational domain, velocity profile and scalar profile is shown in Fig. 1. The original mesh is inhomogeneous in the normal direction. In order to avoid the non-commutativity described in Sec. 2, interpolation is done in normal direction by using Chebyshev polynomial, and a uniform mesh of $192 \times 300 \times 96$ grids is obtained for the following *A Priori* tests. Homogeneous tophat filter is employed in physical space. The grid size is denoted as Δ and the filter size is Δ_f, in each direction respectively. The grid sizes of DNS are the same between streamwise direction and spanwise direction, but smaller in normal direction, since normal direction requires more grids in calculation.

In Fig. 2, our DNS results are compared with the DNS results of Kawamura [26]. The scalar profiles are in quite good agreement, both in the near wall region and the channel center. The scalar variance $\langle\theta^2\rangle$ are also in agreement, except some difference far from wall. This might stem from the lack of grids by employing Chebyshev sample-point method in the normal direction. However, in this paper attention is mainly paid to the near-wall region, where the inhomogeneous effect could cause the rapid terms and our results show good statistical profiles.

The profiles of scalar flux are shown in Fig. 3. In the present case, the scalar flux is positive in the streamwise direction, and negative in the normal direction. In the spanwise direction it is approximately zero. Note that the sign of the value depends on the direction of the coordinate axis. This figure will be needed in the following parts when we analyze the subgrid flux transfer.

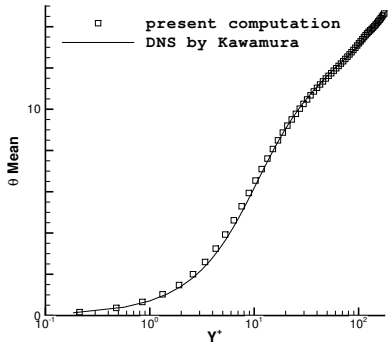

(a) Scalar profile

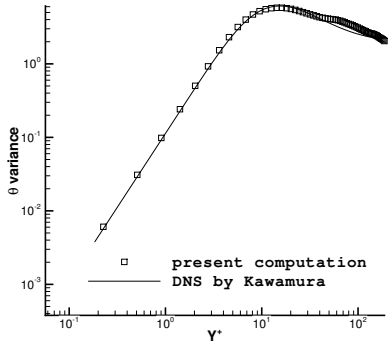

(b) Scalar variance

FIGURE 2. Comparison between two DNS results. Symbols: DNS with pseudo-spectral method; lines: DNS by Kawamura.

4.1 Vector level analysis of rapid and slow subgrid scalar flux

As explained in Sec. 3, the subgrid scalar flux is split into rapid and slow parts. Furthermore, the mean and fluctuating parts are defined. In the following, *A Priori* tests are made to study the behavior of rapid and slow subgrid scalar flux. In the evaluations, we use the Euclidean norm of overall scalar flux $\Pi_\theta = \|\langle \boldsymbol{u}\theta \rangle\|$ to normalize each flux components.

4.1.1 Mean subgrid flux magnitude and its anisotropy Figure 4(a) shows the components of the subgrid flux in streamwise direction, *i.e.* $\tau_{\theta 1}^{rapid}$ and $\tau_{\theta 1}^{slow}$, for different filter sizes Δ_f varying from 2Δ to 8Δ. Note that the rapid part exists mostly in the near-wall region, especially in the region $Y^+ < 10$, where it can be larger than the slow part. And in the center part of Couette flow, the rapid part is negligible because of the nearly homogeneous velocity and scalar fields in this region.

From Eq. (31), the mean rapid part can be rescaled by the filter size $(\Delta_f/\Delta)^2$, and the results are shown in Fig. 4(b). The

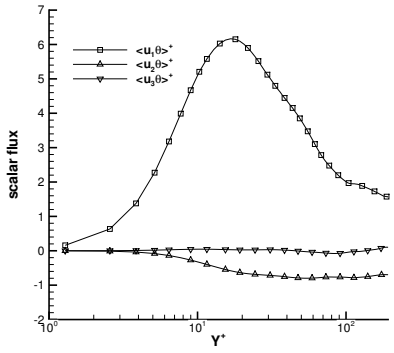

FIGURE 3. Scalar flux profiles.

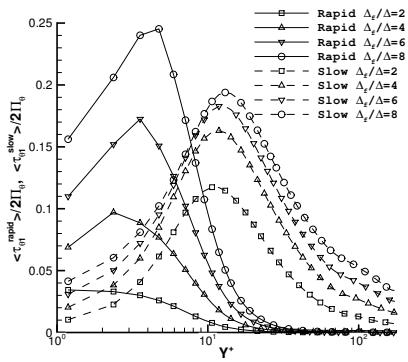

(a) Rapid and slow parts of $\langle \tau_{\theta 1} \rangle$

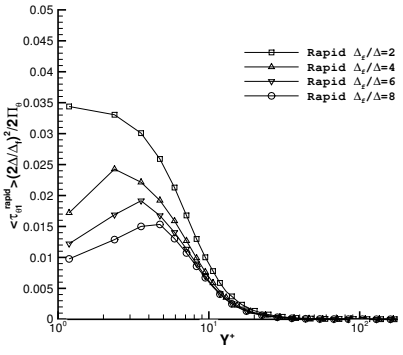

(b) Rapid part of $\langle \tau_{\theta 1} \rangle$, rescaled by the filter size

FIGURE 4. Normalized mean SGS flux components in streamwise direction, $\langle \tau_{\theta 1}/2\Pi_\theta \rangle$, with $\Delta_f/\Delta = 2, 4, 6$, and 8. Solid lines: rapid parts. Dashed lines: slow parts.

scaling law of Eq. (31) is reasonably satisfied in the region $Y^+ > 7$, where the normalized curves tend to collapse.

Another important observation that should be noticed is the strong anisotropy of the mean rapid subgrid scalar flux $\langle \tau_{\theta j}^{rapid} \rangle$. The rapid parts in different directions are shown in Fig. 5(a), where the filter size is fixed at 4Δ. As mentioned in Eq. (31), the only significant component of the rapid mean SGS flux is $\langle \tau_{\theta 1}^{rapid} \rangle$, and other components are equal to zero since $\langle u_2 \rangle = \langle u_3 \rangle = 0$. This is simply because of the scalar and velocity profiles are in the x_1 direction.

The components of the mean slow subgrid scalar flux $\langle \tau_{\theta j}^{slow} \rangle$ are shown in Fig. 5(b). The results show strong anisotropy among the three directions. The differences could also stem from the effect of mean flow and scalar. In streamwise direction, the scalar flux is positive and very strong. In normal direction, the scalar flux is negative and not strong in near-wall region, for instance $Y^+ < 10$. The values in spanwise direction are almost zero. These behaviors are similar as the total scalar flux (Fig. 3).

Thus we could say that the mean flow could affect the mean slow SGS scalar flux mainly in streamwise direction and in $Y^+ < 10$ region. However, in the channel center, there are also anisotropic contributions on the mean slow subgrid scalar flux. The negative values occur in normal direction. Note that the negative subgrid scalar flux does not mean backscatter, as the scalar flux is negative. The analysis of scalar variance will be shown in section 4.2.

4.1.2 Fluctuating subgrid scalar flux magnitude and its anisotropy The root-mean-square (*rms*) value of the subgrid scalar flux is closely related to the behavior of the small scales. Figure 6 shows the *rms* values of normalized subgrid scalar flux components in streamwise direction. The filter sizes are $2\Delta, 4\Delta, 6\Delta$ and 8Δ, respectively. The magnitude of *rms* values of rapid and slow parts are compared. Unlike the mean values in Fig. 4, the slow parts of *rms* values are also large in near-wall region, especially when the filter size is large. The near-wall effect could stem from the strong inhomogeneity of velocity and scalar under spatial filters. In addition, the *rms* values of rapid parts have a similar behavior than their mean counterparts (see Fig. 4).

In order to investigate the anisotropy of fluctuating subgrid scalar flux, Fig. 7 shows the *rms* values of all components of the rapid and slow subgrid scalar flux, for the case with $\Delta_f/\Delta = 4$. Among the rapid components in Fig. 7(a), the most important contribution is in streamwise direction, and the component in normal direction is almost zero. Comparing with Fig. 5(a), there is also the fluctuating contribution in spanwise direction, although the mean value is almost zero. In Fig. 7(b), the three components of *rms* values of the slow subgrid scalar flux are not zero. They have close values in channel center. In the near-wall region ($Y^+ < 20$), the contributions of both rapid and slow *rms*

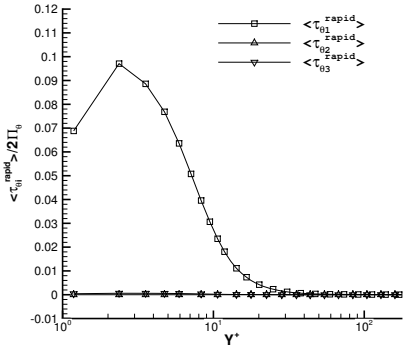

(a) Components of $\langle \tau_{\theta j}^{rapid} \rangle$

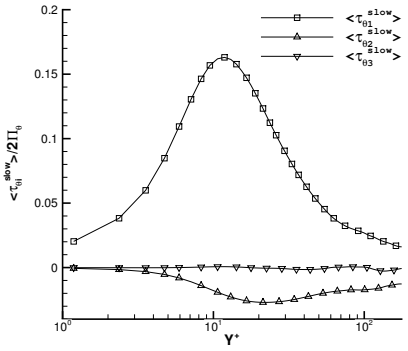

(b) Components of $\langle \tau_{\theta j}^{slow} \rangle$

FIGURE 5. Components of the rapid and slow parts of scalar flux, with $\Delta_f/\Delta = 4$

values are mainly in the streamwise direction.

4.2 Rapid and slow scalar dissipation in the equations of scalar variance

In Sec. 2.1, the governing equations of scalar variance were already derived. The SGS scalar flux are connected with the scalar gradient vector by an inner product, which can be regarded as SGS scalar dissipation. In the following part, the rapid and slow parts of SGS scalar dissipation are studied. The subgrid terms are normalized by using the overall scalar dissipation $\varepsilon_\theta = \kappa \left\langle \frac{\partial \theta}{\partial x_j} \frac{\partial \theta}{\partial x_j} \right\rangle$.

4.2.1 Subgrid dissipation of mean scalar variance

In the governing equation of resolved mean scalar variance (8),

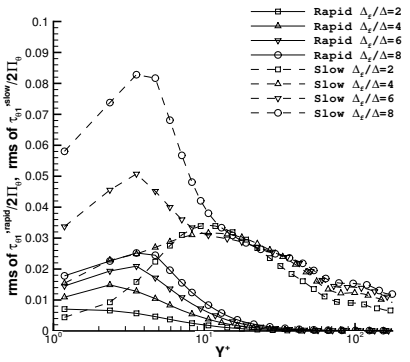

FIGURE 6. Rms of normalized SGS flux components in streamwise direction, $\langle \tau'_{\theta 1}/2k \rangle$, with $\Delta_f/\Delta = 2, 4, 6$, and 8. Solid lines: rapid parts. Dashed lines: slow parts.

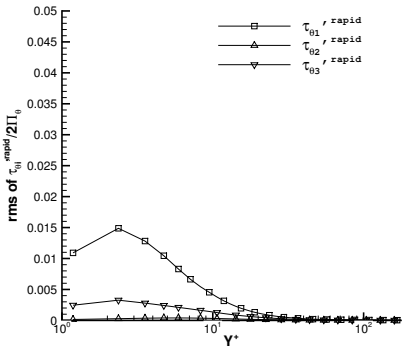

(a) Components of $\tau_{\theta i}^{\prime rapid}$

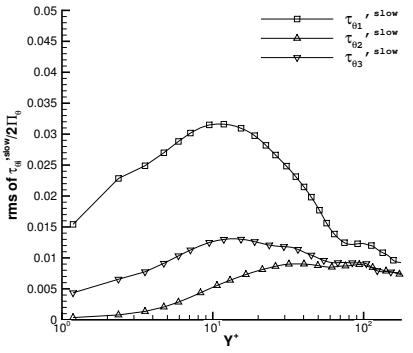

(b) Components of $\tau_{\theta i}^{\prime slow}$

FIGURE 7. Rms of the components of the rapid and slow parts of scalar flux, with $\Delta_f/\Delta = 4$.

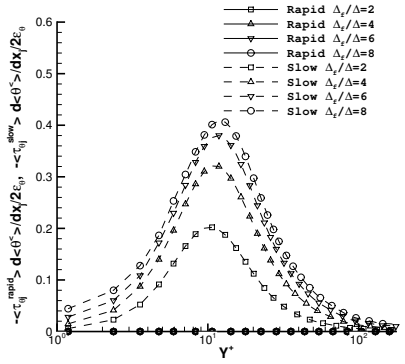

FIGURE 8. Contribution of subgrid dissipation in the transport equation of mean scalar variance, with $\Delta_f/\Delta = 2,4,6$, and 8. Solid lines: rapid parts. Dashed lines: slow parts.

the subgrid term can be decomposed into rapid and slow parts:

$$\left\langle \tau_{\theta j} \right\rangle \frac{\partial \left\langle \theta^{<} \right\rangle}{\partial x_j} = \left\langle \tau_{\theta j}^{rapid} \right\rangle \frac{\partial \left\langle \theta^{<} \right\rangle}{\partial x_j} + \left\langle \tau_{\theta j}^{slow} \right\rangle \frac{\partial \left\langle \theta^{<} \right\rangle}{\partial x_j}, \qquad (32)$$

which are shown in Fig. 8. The filter sizes are $2\Delta, 4\Delta, 6\Delta$ and 8Δ, respectively. In parallel to the observation at the vector level comparison, the contribution of the mean rapid part, $-\left\langle \tau_{\theta j}^{rapid} \right\rangle \frac{\partial \left\langle \theta^{<} \right\rangle}{\partial x_j}$, is zero, because the subgrid flux $\left\langle \tau_{\theta j}^{rapid} \right\rangle$ only has non-zero value when $j = 1$, and the scalar gradient $\frac{\partial \left\langle \theta^{<} \right\rangle}{\partial x_j}$ only has non-zero value when $j = 2$. The mean slow part has non-zero values. Although the value of subgrid scalar flux in normal direction is negative in Fig. 5(b), the value of scalar dissipation is positive, which means that the mean scalar variance is mainly dissipated in subgrid scales.

4.2.2 Subgrid dissipation of fluctuating scalar variance In LES, SGS models aim at simulating the subgrid dissipation of fluctuating scalar variance. In the governing equation of resolved fluctuating scalar variance (9), the subgrid term can be decomposed as

$$\left\langle \tau'_{\theta j} \frac{\partial \theta'^{<}}{\partial x_j} \right\rangle = \left\langle \tau'^{rapid}_{\theta j} \frac{\partial \theta'^{<}}{\partial x_j} \right\rangle + \left\langle \tau'^{slow}_{\theta j} \frac{\partial \theta'^{<}}{\partial x_j} \right\rangle. \qquad (33)$$

The results of this decomposition are shown in Fig. 9(a), comparing with the same decomposition in velocity field shown in Fig. 9(b). (For the rapid-slow decomposition of velocity field, see Ref. [16].) The rapid contributions are mostly in the near-wall region, i.e. $Y^+ < 10$, and they are small in the quasi-homogeneous

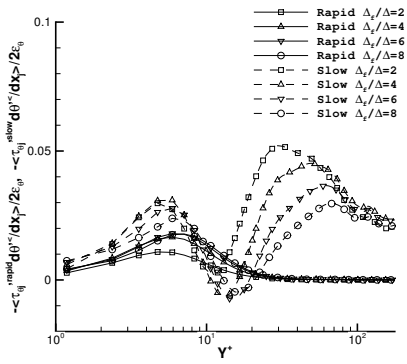

(a) scalar

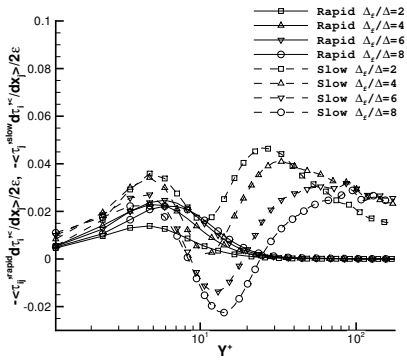

(b) velocity

FIGURE 9. Contribution of subgrid dissipation in subgrid velocity and scalar transport equations, with $\Delta_f/\Delta = 2,4,6$, and 8. Solid lines: rapid parts. Dashed lines: slow parts. (a) scalar (b) velocity.

region near center of channel. The slow fluctuating scalar dissipation, however, has special behavior in the buffer layer, *i.e.* there are negative values in the region $10 < Y^+ < 20$. This means that backscatter is present in this region. This observation is in agreement with the investigations of Hartel *et al.* [5] and Xu [39], which show strong effect of backscatter of velocity field also in this region. This phenomenon might stem from the turbulent structures in buffer layer. In velocity field the backscatter exists when $\Delta_f/\Delta > 4$, while in scalar field $\Delta_f/\Delta > 2$, this difference may indicate the different characteristic scales between velocity and scalar fields, similar as discussed in Cui *et al.* [40] and in [41], among the others. We may also explain this difference by non-local triad interactions of scalar turbulence [42]. The results in Fig. 9 will be compared will SGS models in Sec. 5.

4.3 Rapid and slow scalar transport in the equations of scalar flux

In Sec. 2.2, the governing equations of scalar flux were derived. In those equations, subgrid interactions exist between SGS scalar flux and velocity gradient tensor, as well as between subgrid stress tensor and scalar gradient vector. The former represents the interaction between GS velocity and SGS scalar; while the latter represents the interaction between GS scalar and SGS velocity. In order to study these contributions, we would like to introduce Yeung's work. Yeung splits scalar variance transfer term into four parts in spectral space [43]:

1. The interaction between GS velocity and GS scalar (GVGS). It causes GS transfer.
2. The interaction between GS velocity and SGS scalar (GVSS). It causes SGS transfer.
3. The interaction between SGS velocity and GS scalar (SVGS). It causes SGS transfer.
4. The interaction between SGS velocity and SGS scalar (SVSS). It causes SGS transfer.

Among the three parts causing SGS transfer (GVSS, SVGS, and SVSS), the interaction between GS velocity and SGS scalar (GVSS) is the main part, which is much more strong than the other two parts. In particular, GVSS is usually compared with SVGS since they both involve GS variables, and GVSS has much more contribution than SVGS has. This phenomenon was verified in isotropic scalar turbulence by Yeung [43] and in anisotropic scalar turbulence by Fang [42]. In the following part, we would like to investigate this phenomenon in the transport of scalar flux in inhomogeneous anisotropic channel flow, with a spatial filter in physical space. Besides, we will also study the effect of rapid parts, which has not been investigated yet. The subgrid terms are normalized by using the Euclidean norm of overall scalar flux $\varepsilon_{u\theta} = (\nu+\kappa)\left\|\frac{\partial \boldsymbol{u}}{\partial x_j}\frac{\partial \theta}{\partial x_j}\right\|$.

4.3.1 Subgrid transport of mean scalar flux

There are two subgrid dissipation terms in the transport equation of resolved mean scalar flux (15), which could be denoted as $\left\langle \tau_{\theta j}\right\rangle \dfrac{\partial \left\langle u_i^<\right\rangle}{\partial x_j}$ and $\left\langle \tau_{ij}\right\rangle \dfrac{\partial \left\langle \theta^<\right\rangle}{\partial x_j}$. They can be decomposed into rapid and slow parts, respectively as follows:

$$\begin{aligned}\left\langle \tau_{\theta j}\right\rangle \frac{\partial \left\langle u_i^<\right\rangle}{\partial x_j} &= \left\langle \tau_{\theta j}^{rapid}\right\rangle \frac{\partial \left\langle u_i^<\right\rangle}{\partial x_j} + \left\langle \tau_{\theta j}^{slow}\right\rangle \frac{\partial \left\langle u_i^<\right\rangle}{\partial x_j},\\ \left\langle \tau_{ij}\right\rangle \frac{\partial \left\langle \theta^<\right\rangle}{\partial x_j} &= \left\langle \tau_{ij}^{rapid}\right\rangle \frac{\partial \left\langle \theta^<\right\rangle}{\partial x_j} + \left\langle \tau_{ij}^{slow}\right\rangle \frac{\partial \left\langle \theta^<\right\rangle}{\partial x_j},\end{aligned} \tag{34}$$

where the rapid and slow parts of subgrid stress τ_{ij} are defined similar as the subgrid scalar flux $\tau_{\theta j}$. The details can be found in Shao's paper [16].

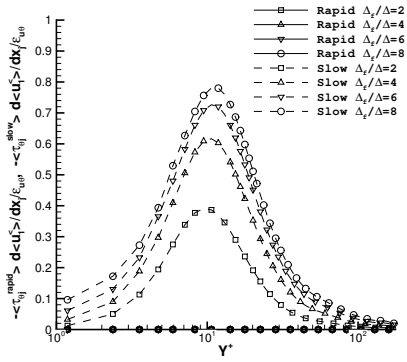

(a) $\left\langle \tau_{\theta j}^{rapid}\right\rangle \dfrac{\partial \left\langle u_1^<\right\rangle}{\partial x_j}$ and $\left\langle \tau_{\theta j}^{slow}\right\rangle \dfrac{\partial \left\langle u_1^<\right\rangle}{\partial x_j}$

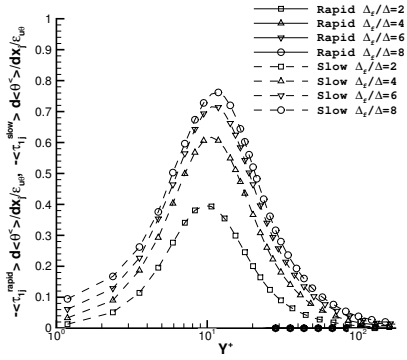

(b) $\left\langle \tau_{1j}^{rapid}\right\rangle \dfrac{\partial \left\langle \theta^<\right\rangle}{\partial x_j}$ and $\left\langle \tau_{1j}^{slow}\right\rangle \dfrac{\partial \left\langle \theta^<\right\rangle}{\partial x_j}$

FIGURE 10. Contribution of subgrid transport in mean scalar flux equation, at $\Delta_f/\Delta = 2,4,6$, and 8. Solid lines: rapid parts. Dashed lines: slow parts.

These four terms are shown in Fig. 10. Note that in the mean scalar flux equation, only the component in streamwise direction, *i.e.* $\left\langle u_1^<\right\rangle \left\langle \theta^<\right\rangle$, is not equal to zero. All the rapid terms have zero values. Between Figs. 10(a) and 10(b), the magnitudes of the slow terms are almost the same. It shows that the contribution on mean scalar flux of GS velocity and SGS scalar is almost the same as the contribution of SGS velocity and GS scalar. It is reasonable since in Eq. (31), the magnitude of rapid subgrid is expressed by the mean gradients of velocity and scalar. We could similarly write the expression for subgrid stress, using the same method as in Sec. 3.1, finally the terms are of the same magnitude between Figs. 10(a) and 10(b). In addition, in both figures the subgrid transfer increases when the filter size increases.

4.3.2 Subgrid transport of fluctuating scalar flux

Similarly, there are two subgrid dissipation terms in the trans-

port equation of resolved fluctuating scalar flux (16), which are $\left\langle \tau'_{\theta j} \frac{\partial u'^{<}_i}{\partial x_j} \right\rangle$ and $\left\langle \tau'_{ij} \frac{\partial \theta'^{<}}{\partial x_j} \right\rangle$. They could be decomposed into rapid and slow parts, respectively:

$$\begin{aligned} \left\langle \tau'_{\theta j} \frac{\partial u'^{<}_i}{\partial x_j} \right\rangle &= \left\langle \tau'^{rapid}_{\theta j} \frac{\partial u'^{<}_i}{\partial x_j} \right\rangle + \left\langle \tau'^{slow}_{\theta j} \frac{\partial u'^{<}_i}{\partial x_j} \right\rangle, \\ \left\langle \tau'_{ij} \frac{\partial \theta'^{<}}{\partial x_j} \right\rangle &= \left\langle \tau'^{rapid}_{ij} \frac{\partial \theta'^{<}}{\partial x_j} \right\rangle + \left\langle \tau'^{slow}_{ij} \frac{\partial \theta'^{<}}{\partial x_j} \right\rangle. \end{aligned} \tag{35}$$

These four terms are shown in Figs. 11-13, in different directions respectively. Each figure on the left denotes the GVSS contribution, while on the right represents the SVGS part. Similar as analyzed before, the rapid parts mainly exist in the streamwise direction, and are almost zero in normal and spanwise direction. For the slow parts in the streamwise direction, in the region $10 < Y^+ < 20$ there is also backscatter, which is similar as the analysis of energy variance. Both GVSS and SVGS terms show the same behavior. For the slow parts in the normal direction, GVSS term has negative value while SVGS term is positive in most part of the channel. Since the total scalar flux is negative (see Fig. 3), here GVSS term is the forward transfer and SVGS term is backscatter. This behavior of backscatter is quite obvious in the region $Y^+ \simeq 20$. All terms of the slow parts in the spanwise direction are almost zero.

We then focus on the mostly homogeneous region ($Y^+ > 100$), the principal contribution among the six figures is the GVSS term in streamwise direction, i.e. Fig. 11(a). It is much stronger than the SVGS term in the same direction, i.e. Fig. 11(b). This phenomenon is in agreement with the results of Yeung [43] and Fang [42]. Thus in the homogeneous anisotropic region, the GVSS term could be considered as the major contribution of subgrid scalar flux.

5 A Priori evaluation of subgrid models

From the discussion in the previous sections, it is clear that, through the rapid part, the mean velocity and scalar gradient directly affects the SGS scalar flux and the associated scalar transfer to the small scales. The question that then arises is whether SGS modeling has to explicitly account for the effect of the mean velocity and scalar gradient manifested by the rapid SGS stress. In fact, since the rapid SGS scalar flux strongly depends on the type of filter, and only exists in inhomogeneous scalar turbulence, it can not be represented by most of the SGS models. Scale-similarity model (SSM) is one of the only models related to filter. Thus in the following part, we follow Shao's conclusion [16], to represent the rapid parts by using SSM:

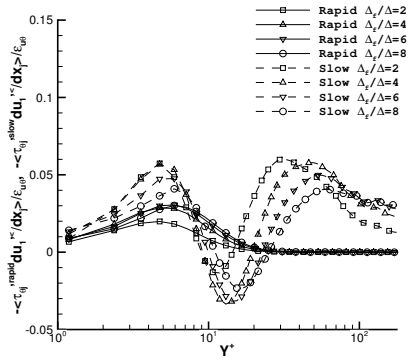

(a) $\left\langle \tau'^{rapid}_{\theta j} \frac{\partial u'^{<}_1}{\partial x_j} \right\rangle$ and $\left\langle \tau\theta j'^{slow} \frac{\partial u'^{<}_1}{\partial x_j} \right\rangle$

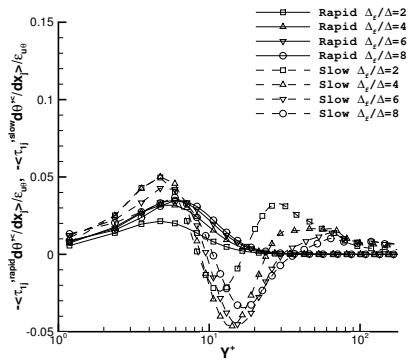

(b) $\left\langle \tau'^{rapid}_{1j} \frac{\partial \theta'^{<}}{\partial x_j} \right\rangle$ and $\left\langle \tau'^{slow}_{1j} \frac{\partial \theta'^{<}}{\partial x_j} \right\rangle$

FIGURE 11. The contribution of subgrid transport in resolved scalar flux equation, in the streamwise direction, with $\Delta_f/\Delta = 2, 4, 6$, and 8. Solid lines: rapid parts. Dashed lines: slow parts. (a) GVSS term. (b) SVGS term.

$$\begin{aligned} \tau'^{rapid}_{\theta j} =& C_m \Big[\left(\langle\theta\rangle^{<} \langle u_j \rangle^{<} \right)^{<} - \langle\theta\rangle^{<<} \langle u_j \rangle^{<<} + \left(\langle\theta\rangle^{<} \langle u_j \rangle^{<} \right)^{<} \\ & - \langle\theta\rangle^{<<} u'^{<<}_j + \left(\theta'^{<} \langle u_j \rangle^{<} \right)^{<} - \theta'^{<<} \langle u_j \rangle^{<<} \Big], \end{aligned} \tag{36}$$

where the coefficient $C_m = 1$. The second filter operation is done with a "test" filter that is the same as the original "grid" top-hat filter.

Besides, in order to simulate the slow subgrid scalar dissipation, we apply the eddy-diffusivity assumption with constant turbulent Prandtl number, which can be written as

$$\tau'^{slow}_{\theta j} = -\kappa_t \frac{\partial \theta'^{<}}{\partial x_j}, \qquad \kappa_t = \frac{\nu_t}{\mathrm{Pr}_t}. \tag{37}$$

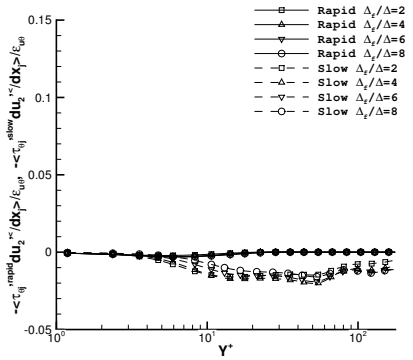

(a) $\left\langle \tau_{\theta j}^{\prime rapid} \dfrac{\partial u_2^{\prime <}}{\partial x_j} \right\rangle$ and $\left\langle \tau\theta j^{\prime slow} \dfrac{\partial u_2^{\prime <}}{\partial x_j} \right\rangle$

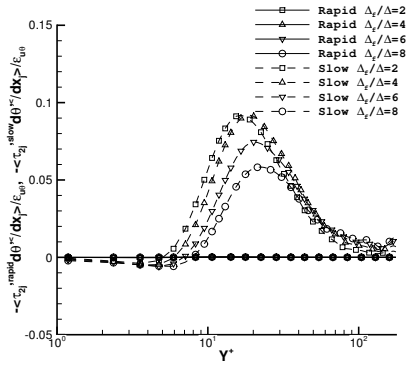

(b) $\left\langle \tau_{2j}^{\prime rapid} \dfrac{\partial \theta^{\prime <}}{\partial x_j} \right\rangle$ and $\left\langle \tau_{2j}^{\prime slow} \dfrac{\partial \theta^{\prime <}}{\partial x_j} \right\rangle$

FIGURE 12. The contribution of the subgrid transport in the resolved scalar flux equation, in the normal direction, with $\Delta_f/\Delta = 2,4,6$, and 8. Solid lines: rapid parts. Dashed lines: slow parts. (a) GVSS term. (b) SVGS term.

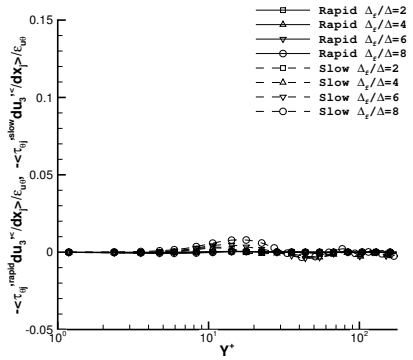

(a) $\left\langle \tau_{\theta j}^{\prime rapid} \dfrac{\partial u_3^{\prime <}}{\partial x_j} \right\rangle$ and $\left\langle \tau\theta j^{\prime slow} \dfrac{\partial u_3^{\prime <}}{\partial x_j} \right\rangle$

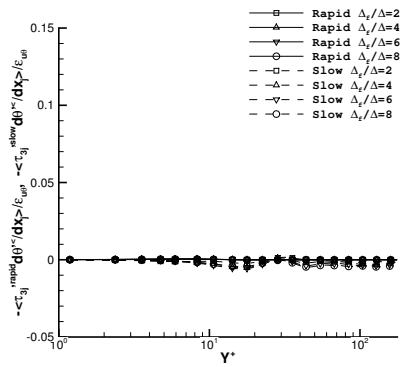

(b) $\left\langle \tau_{3j}^{\prime rapid} \dfrac{\partial \theta^{\prime <}}{\partial x_j} \right\rangle$ and $\left\langle \tau_{3j}^{\prime slow} \dfrac{\partial \theta^{\prime <}}{\partial x_j} \right\rangle$

FIGURE 13. The contribution of the subgrid transport in the resolved scalar flux equation, in the span direction, with $\Delta_f/\Delta = 2,4,6$, and 8. Solid lines: rapid parts. Dashed lines: slow parts. (a) GVSS term. (b) SVGS term.

ν_t is computed using two classical models. One is the Smagorinsky model $\nu_t = (C_s\Delta)^2(2|S_{ij}^{\prime <}S_{ij}^{\prime <}|)^{1/2}$ with $C_s = 0.1$ and with van Driest damping function in near-wall region (SM damping). Another is the Germano Dynamic Smagorinsky model (DSM) [4]. In both cases the turbulent Prandtl number is fixed as $\mathrm{Pr}_t = \mathrm{Pr}$. The subgrid scalar dissipation is calculated and compared with exact slow values, and is shown in Fig. 14(a). For comparison, we also show the same result in velocity field, in Fig. 14(b). It is found that the models can not represent the bumps around $Y^+ = 5$. This problem exists in both velocity and scalar fields, and can not be simply improved. In another paper of authors, more models have been tested (see Fig. 3 of Ref. [44]), the same phenomenon is also observed. In other regions, SGS models have good agreement with exact slow energy dissipation in velocity field, as investigated by Shao *et al.* [16], but they agree not well in scalar field. In channel center they do not dissipate enough, and around $Y^+ = 15$ they can not show the backscatter of scalar variance. In order to propose a better SGS scalar model, we choose a more accurate anisotropic model by Cui *et al.* (Cui Model) [31] to represent the slow parts. Comparing with other SGS models, this anisotropic model explicitly represents the eddy diffusion as a function of mean velocity and scalar, which can be related with the rapid-slow analysis in this paper.

5.1 Extended formulation of Cui Model

The original subgrid scalar model in Ref. [31] did not consider the mean scalar gradient. In this section we consider that the turbulence is homogeneous with mean shear γ and mean scalar gradient G, thus the velocity and scalar can be decomposed to mean and fluctuation as: $u_i = u_i' + \gamma x_2 \delta_{i1}, \theta = \theta' + G x_2$. The equation of large eddy simulation for scalar turbulence can

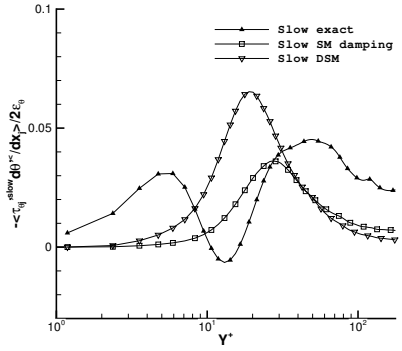

(a) scalar

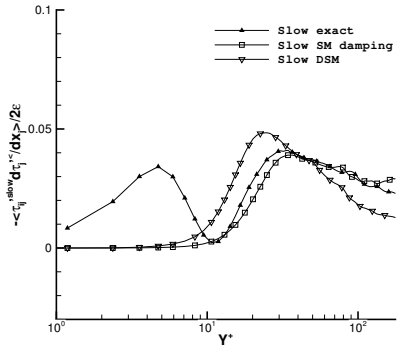

(b) velocity

FIGURE 14. Comparison between exact values and model values. $\Delta_f/\Delta = 4$. Smagorinsky model with constant turbulent Prandtl number is applied. (a) scalar (b) velocity.

then be written as

$$\frac{\partial \theta'^{<}}{\partial t} + \left(u_j'^{<} + \gamma x_2 \delta_{j1}\right)\left(\frac{\partial \theta'^{<}}{\partial x_j} + G\delta_{j2}\right) = \kappa \frac{\partial^2 \theta'^{<}}{\partial x_j \partial x_j} - \frac{\partial \tau'_{\theta j}}{\partial x_j}. \tag{38}$$

Following the same process as in Ref. [31], defining the structure functions $D^{<}_{\theta\theta} = \left\langle \delta\theta'^2 \right\rangle, D^{<}_{j\theta\theta} = \left\langle \delta u_j'^{<} \delta\theta'^2 \right\rangle$ and $D^{<}_{2\theta} = \left\langle \delta u_2'^{<} \delta\theta' \right\rangle$, neglecting the molecular diffusivity, and making average in a local sphere of radius r, finally the SGS eddy diffusivity can be obtained as (Extended Cui Model, denoted as ECM)

$$\kappa_t = \frac{6\left(D^{<}_{r\theta\theta}\right)^A + 6\gamma r\left(D^{<}_{\theta\theta} n_1 n_2\right)^A + \left(D^{<}_{2\theta}\right)^V Gr}{6\left(\dfrac{dD^{<}_{\theta\theta}}{dr}\right)^A - 4r\left\langle \dfrac{\partial \theta'^{<}}{\partial x_j}\dfrac{\partial \theta'^{<}}{\partial x_j} \right\rangle^V} \tag{39}$$

in which the notations $(\bullet)^A$ and $(\bullet)^V$ are local surface average and local volume average. We can also divide it into two parts:

$$\begin{aligned} \kappa_t^{fs} &= \frac{6\left(D^{<}_{r\theta\theta}\right)^A}{6\left(\dfrac{dD^{<}_{\theta\theta}}{dr}\right)^A - 4r\left\langle \dfrac{\partial \theta'^{<}}{\partial x_j}\dfrac{\partial \theta'^{<}}{\partial x_j} \right\rangle^V}, \\ \kappa_t^{ms} &= \frac{6\gamma r\left(D^{<}_{\theta\theta} n_1 n_2\right)^A + \left(D^{<}_{2\theta}\right)^V Gr}{6\left(\dfrac{dD^{<}_{\theta\theta}}{dr}\right)^A - 4r\left\langle \dfrac{\partial \theta'^{<}}{\partial x_j}\dfrac{\partial \theta'^{<}}{\partial x_j} \right\rangle^V}, \end{aligned} \tag{40}$$

in which κ_t^{fs} represents only the interactions of subgrid scale (fluctuating part), and κ_t^{ms} contains the informations of mean flow and mean scalar (mean part), *i.e.* γ and G, explicitly. Comparing with the original model formulation in Ref. [31], mean scalar gradient is additionally considered. Because only homogeneous velocity and scalar fields are considered in Eq. (38), we consider that ECM only simulates the slow SGS scalar flux. However, this model formulation shows that the slow SGS scalar flux is not only affected by SGS fluctuations, but also relative with the mean profiles. The ECM can be regarded as a good supplement to the slow part SGS of the rapid-slow analysis in this paper.

5.2 Evaluation of subgrid scalar dissipation

From Eq. (40), subgrid eddy-diffusivity is split into mean and fluctuating parts. Thus from eddy-diffusivity assumption, the mean and fluctuating subgrid scalar flux are expressed as [5]:

$$\tau'^{ms}_{\theta j} = -\kappa_t^{ms}\frac{\partial \theta'}{\partial x_j}, \qquad \tau'^{fs}_{\theta j} = -\kappa_t^{fs}\frac{\partial \theta'}{\partial x_j}. \tag{41}$$

The relative terms of subgrid scalar dissipation read

$$\begin{aligned} \left\langle \tau'^{ms}_{\theta j}\frac{\partial \theta'^{<}}{\partial x_j} \right\rangle &= \kappa_t^{ms}\left\langle \frac{\partial \theta'^{<}}{\partial x_j}\frac{\partial \theta'^{<}}{\partial x_j} \right\rangle, \\ \left\langle \tau'^{fs}_{\theta j}\frac{\partial \theta'^{<}}{\partial x_j} \right\rangle &= \kappa_t^{fs}\left\langle \frac{\partial \theta'^{<}}{\partial x_j}\frac{\partial \theta'^{<}}{\partial x_j} \right\rangle. \end{aligned} \tag{42}$$

With an ideal subgrid model, there should be

$$\begin{aligned} \tau'^{slow}_{\theta j} &= \tau'^{ms}_{\theta j} + \tau'^{fs}_{\theta j}, \\ \left\langle \tau'_{\theta j}\frac{\partial \theta'^{<}}{\partial x_j} \right\rangle &= \left\langle \tau'^{ms}_{\theta j}\frac{\partial \theta'^{<}}{\partial x_j} \right\rangle + \left\langle \tau'^{fs}_{\theta j}\frac{\partial \theta'^{<}}{\partial x_j} \right\rangle. \end{aligned} \tag{43}$$

The mean and fluctuating parts of subgrid scalar dissipation are shown in Fig. 15, by employing ECM. The filter sizes are

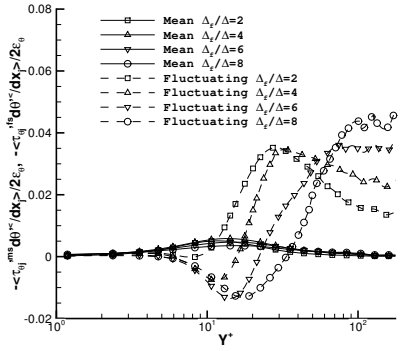

FIGURE 15. Mean and fluctuating parts in the ECM, with $\Delta_f/\Delta = 2,4,6$, and 8. Solid lines: mean parts. Dashed lines: fluctuating parts.

$2,4,6$ and 8 times of grid size, respectively. We would like emphasize that here mean and fluctuating parts are both slow contribution due to the effect on slow scalar dissipation by mean velocity and scalar. The mean part has positive values but small comparing with the fluctuating part, which means that slow scalar variance is weakly dissipated by mean velocity and mean scalar. The peak locations is about $Y^+ \simeq 15$. The fluctuating part has the main contribution. It is positive in most region of channel, which means that in most region scalar variance is dissipated. In channel center, flow is almost homogeneous, and subgrid dissipation increases when filter size increases. However, there are also negative values around the $Y^+ \simeq 15$ range, *i.e.* the buffer layer. Comparing with the model behaviors in Fig. 14, where classical models always dissipate, we could regard the backscatter property as an advantage of ECM.

The following work is introducing SSM for rapid SGS scalar flux, as was discussed before. The total slow subgrid scalar dissipation is calculated by employing the total eddy diffusivity $\kappa_t = \kappa_t^{ms} + \kappa_t^{fs}$. SSM is used to simulate the rapid subgrid scalar dissipation. With different filter size, the comparisons between exact values and modeled values are shown in Fig. 16, respectively.

For the slow parts of subgrid scalar dissipation, the model results have similar behavior as the exact values. In channel center, where the turbulence is almost homogeneous, their magnitudes are in good agreement, especially when Δ_f equal to 4Δ and 6Δ. In near-wall region, all model values are smaller than exact values, which means that ECM does not dissipate enough in the viscous sublayer. Comparing with the results of SM and DSM in Fig. 14, there is no improvement in this range. It could really be a serious problem for large-eddy simulation as noticed by Spalart [45]. However, an advantage could be found in the ECM, that in buffer layer ($Y^+ \simeq 15$), the behavior of scalar backscatter is well simulated. The peak locations and values of ECM are

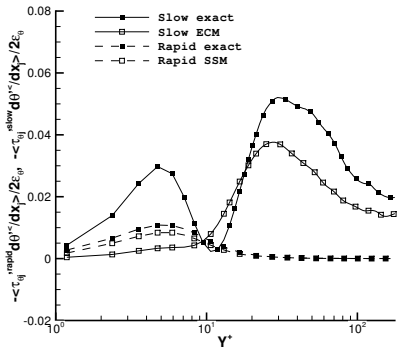

(a) $\Delta_f = 2\Delta$

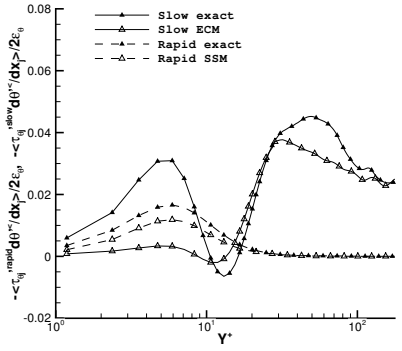

(b) $\Delta_f = 4\Delta$

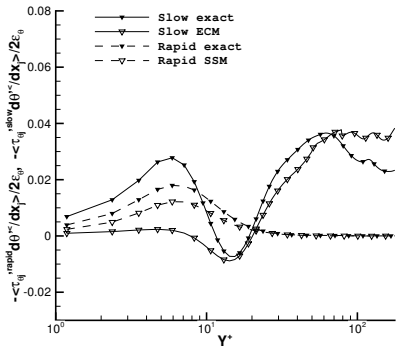

(c) $\Delta_f = 6\Delta$

FIGURE 16. Comparison between exact and model values of scalar dissipation, with $\Delta_f/\Delta = 2,4$, and 6. Solid line and filled symbols: exact value of slow subgrid scalar dissipation. Solid line and hollow symbols: slow subgrid scalar dissipation by using the shear model. Dashed line and filled symbols: exact value of rapid subgrid scalar dissipation. Dashed line and hollow symbols: rapid subgrid scalar dissipation by using scale-similarity model on the velocity and scalar profiles.

in quite good agreement with the exact results. In brief, both the agreements in channel center and in the range of backscatter could be considered as an improvement than other scalar models. For the rapid parts, the scale-similarity model simulates quite well the strong dissipation in near-wall region.

Therefore, we propose ECM to be employed in wall-bounded scalar turbulence. It could represent the behavior of subgrid scalar backscatter. The mean velocity and scalar profiles could affect the subgrid scalar flux explicitly. In addition, in the inhomogeneous region, the SSM could be employed on the mean velocity and scalar, to simulate the "rapid" part of subgrid scalar flux and subgrid dissipation.

6 Conclusion

In application and development of LES, the "rapid-slow" decomposition can be used to investigate the effects of inhomogeneity, of mean flow or large coherent eddies on the subgrid stresses tenor and to evaluate the performance of SGS models. In the present study this decomposition was applied to the case of inhomogeneous scalar turbulence. Usually most studies of SGS models only focus on the slow part and neglect the rapid part, despite its important influence due to the non-uniform mean gradients, as well as to the strong inhomogeneity near the walls. In this paper, the "rapid-slow" decomposition was applied to a turbulent Couette flow with a passive scalar. The influence of the rapid part of SGS was studied for both the scalar variance and the scalar flux. The results were used to evaluate the SGS model behavior, and *A Priori* tests using several SGS scalar models were then performed.

By analytical and numerical analysis, it was found that the magnitude of the rapid SGS scalar flux depends on the gradient of both mean velocity and mean scalar and scales as Δ^2. In the near-wall region, where the inhomogeneity is strong, the rapid part is important. A strong anisotropy in rapid SGS scalar flux was also observed.

In the governing equations of scalar variance and scalar flux, the phenomenon of backscatter was observed in the region $10 < Y^+ < 20$. Similar phenomenon has been observed on velocity field in Hartel *et al.* [5] and Xu [39], but in scalar field results are not exactly the same. This phenomenon might be related to the difference of characteristic scales and the non-local triad interactions. It needs further investigation. The transport of scalar flux was then further splitted into four parts using the approach introduced by Yeung [43]. In the center region of the channel, where the flow is nearly homogeneous, the GVSS part (the interaction between GS velocity and SGS scalar) is found much stronger than the SVGS part (the interaction between SGS velocity and GS scalar). This result is in agreement with the studies of Yeung [43] and Fang [42].

It is of practical interest to determine if existing models can represent the influence of the mean velocity and scalar gradients. Following Shao's result for the velocity field [16], the rapid part was modeled by using the scale-similarity model. Slow part has been evaluated using classical eddy diffusivity SGS model. In velocity field models perform well except the region around $Y^+ = 5$, but in scalar field the eddy diffusivity SGS models fail in representation of slow part in both near wall and center region of the channel. Therefore we introduced an extended scalar SGS model (ECM), in which the mean velocity and scalar are explicitly included. It is found that the ECM can partly well represent the slow SGS scalar dissipation, even on the backscatter at about $Y^+ \simeq 15$. Thus, a combined model with slow and rapid parts modeled separately should be considered in LES applications. A remaining problem is the large dissipation near the wall, which exists in both velocity and scalar fields. None of the SGS models tested in the present paper could represent this effect. This problem requires more investigation in the future.

The present work clarifies the meaning of SGS modeling for inhomogeneous scalar wall turbulence. We point out the importance of the mean velocity and mean scalar in SGS modeling. Most popular SGS models only aim at representing the slow part of SGS scalar flux and fail. Introducing the new ECM model for the slow part partly improves the performance. Note that in order to better account for mean shear effect, several works have been initiated in velocity field [31, 46, 47]. Similar approach is still lacking for scalar turbulence. Besides, the importance of the rapid part of SGS scalar flux is clear in the near-wall region: this part can not be neglected as is usually done in existing SGS models. Representing the rapid part is still difficult for SGS models. We propose to apply the SSM for this part. In summary, the result in this work could shed light in future SGS modeling of LES.

Acknowledgment

L. Shao wishes to express the sincere gratitude to the support from NSFC (Grant No 10828204) and to BUAA SJP 111 program. L. Fang is supported by Chinese Scholarship Council and LIAMA 97-03.

REFERENCES

[1] Piomelli, U., Moin, P., and Ferziger, J., 1988. "Model consistency in large eddy simulation of turbulent channel flows". *Physics of Fluids,* ***31***(7), pp. 1884–1981.

[2] Bardina, J., Ferziger, J., and Reynolds, W., 1987. "Improved subgrid-scale models for large-eddy simulation". *AIAA paper*, pp. 80–1357.

[3] Liu, S., Meneveau, C., and Katz, J., 1994. "On the properties of similarity subgrid-scale models as deduced from measurements in a turbulent jet". *Journal of Fluid Mechanics,* ***275***, p. 83.

[4] Germano, M., Piomelli, U., Moin, P., and Cabot, W., 1991.

"A dynamic subgrid-scale eddy viscosity model". *Physics of Fluids A,* ***3***(7), pp. 1760–1765.

[5] Hartel, C., Kleiser, L., Unger, F., and Friedrich, R., 1994. "Subgrid-scale energy transfer in the near-wall region of turbulent flows". *Physics of Fluids,* ***6***(9), pp. 3130–3143.

[6] Kraichnan, R. H., 1976. "Eddy viscosity in two and three dimensions". *Journal of the Atmospheric Sciences,* ***33***, pp. 1521–1536.

[7] Leslie, D. C., and Quarini, G. L., 1979. "The application of turbulence theory to the formulation of subgrid modeling procedures". *Journal of Fluid Mechanics,* ***91***, p. 75.

[8] Leith, C. E., 1990. "Stochastic backscatter in a subgrid-scale model: Plane shear mixing layer". *Physics of Fluids A,* ***2***, p. 297.

[9] Chollet, J., and Lesieur, M., 1981. "Parametrization of small scales of three-dimensional isotropic turbulence utilizing spectral closures.". *Journal of the Atmospheric Sciences,* ***38***, pp. 2747–2757.

[10] Bertoglio, J. P., and Mathieu, J., 1984. "A stochastic subgrid model for large eddy simulation: general formulation". *C. R. Acad. Sci., Ser. II: Mec. Phys., Chim., Sci. Terre Univers,* ***299***, p. 751.

[11] Bertoglio, J. P., 1985. "A stochastic subgrid model for sheared turbulence". In Proceedings of macroscopic modelling of turbulent flows, Lecture notes in physics, Vol.230, pp. 100–119.

[12] Marstorp, L., Brethouwer, G., and Johansson, A. V., 2007. "A stochastic subgrid model with application to turbulent flow and scalar mixing". *Physics of Fluids,* ***19***.

[13] Schumann, U., 1975. "Subgrid scales model for finite difference simulation of turbulent flows in plane channels and annuli". *Journal of Computational Physics,* ***18***, p. 367.

[14] Laporta, A., and Bertoglio, J., 1995. "A model for inhomogeneous turbulence based on two-point correlations". *Advances in turbulence V, Proceedings of the 5th European Turbulence Conference, Siena, Italy*, pp. 286–297.

[15] O'Neil, J., and Meneveau, C., 1997. "Subgrid-scale stresses and their modelling in a turbulent plane wake". *Journal of Fluid Mechanics,* ***349***, p. 253.

[16] Shao, L., Sarkar, S., and Pantano, C., 1999. "On the relationship between the mean flow and subgrid stresses in large eddy simulation of turbulent shear flows". *Physics of Fluids,* ***11***(5), pp. 1229–1248.

[17] Shraiman, B. I., and Siggia, E. D., 2000. "Scalar turbulence". *Nature,* ***405***, p. 639.

[18] Warhaft, Z., 2000. "Passive scalars in turbulent flows". *Annual Review of Fluid Mechanics,* ***32***, pp. 203–240.

[19] Sreenivasan, K. R., 1991. "On local isotropy of passive scalars in turbulent shear flows". *Proceedings of the Royal Society: Mathematical and Physical Sciences,* ***434***(1890), pp. 165–182.

[20] Mestayer, P., 1982. "Local isotropy and anisotropy in a high-reynolds-number turbulent boundary layer". *Journal of Fluid Mechanics,* ***125***, pp. 475–503.

[21] Celani, A., Lanotte, A., Mazzino, A., and Vergassola, M., 2001. "Fronts in passive scalar turbulence". *Physics of Fluids,* ***13***, p. 1768.

[22] Bos, W., Touil, H., Shao, L., and Bertoglio, J., 2004. "On the behavior of the velocity-scalar cross correlation spectrum in the inertial range". *Physics of Fluids,* ***16***(10), pp. 3818–3823.

[23] O'Gorman, P. A., and Pullin, D. I., 2005. "Effect of schmidt number on the velocity-scalar cospectrum in isotropic turbulence with a mean scalar gradient". *Journal of Fluid Mechanics,* ***532***, pp. 111–140.

[24] Bos, W. J. T., and Bertoglio, J., 2007. "Inertial range scaling of scalar flux spectra in uniformly sheared turbulence". *Physics of Fluids,* ***19***, p. 025104.

[25] Kaltenbach, H., Gerz, T., and Schumann, U., 1994. "Large-eddy simulation of homogeneous turbulence and diffusion in stably stratified shear flow". *Journal of Fluid Mechanics,* ***280***, pp. 1–40.

[26] Kawamura, H., Abe, H., and Shingai, K., 2000. "DNS of turbulence and heat transport in a channel flow with different Reynolds and Prandtl numbers and boundary conditions". *Turbulence, Heat and Mass Transfer*.

[27] Jaberi, F., and Collucci, P., 2003. "Large eddy simulation of heat and mass transport in turbulent flows. part 2: scalar field". *International Journal of Heat and Mass Transfer,* ***46***, pp. 1827–1840.

[28] Calmet, I., and Magnaudet, J., 1997. "Large-eddy simulation of high-schmidt number mass transfer in a turbulent channel flow". *Physics of Fluids,* ***9***(2), pp. 438–455.

[29] Wang, W. P., and Pletcher, R., 1997. "On the large eddy simulation of a turbulent channel flow with significant heat transfer". *Physics of Fluids,* ***8***(12), pp. 3354–3366.

[30] GX, W., Vinkovic, I., Shao, L., and Simoëns, S., 2006. "Scalar dispersion by a large-eddy simulation and a lagrangian stochastic subgrid model". *Physics of Fluids,* ***18***(9).

[31] Cui, G., Xu, C., Fang, L., Shao, L., and Zhang, Z., 2007. "A new subgrid eddy-viscosity model for large-eddy simulation of anisotropic turbulence". *Journal of Fluid Mechanics,* ***582***, pp. 377–397.

[32] Ghosal, S., and Moin, P., 1995. "The basic equations of large eddy simulation of turbulent flows in complex geometry". *Journal of Computational Physics,* ***118***, p. 24.

[33] Vasilyev, O., Lund, T., and Moin, P., 1998. "A general class of commutative filters for LES in complex geometries". *Journal of Computational Physics,* ***146***, pp. 82–104.

[34] Marsden, A., and Vasilyev, O., 1999. "Commutative filters for LES on unstructured meshes". *Center for Turbulence Research, Annual Research Briefs*, pp. 389–402.

[35] Rotta, J., 1951. "Statistische theorie nichthomogener tur-

bulenz". *Zeitschrift fr Physik A Hadrons and Nuclei,* ***129***, pp. 547–592.
[36] Lumley, J., 1978. "Computational modeling of turbulent flows". *Advances in applied mechanics,* ***18***, p. 123.
[37] Jimenez, C., Valino, L., and Dopazo, C., 2001. "A priori and a posteriori tests of subgrid scale models for scalar transport". *Physics of Fluids,* ***13***(8), pp. 2433–2436.
[38] Xu, C. X., Zhang, Z. S., and Nieuwstadt, F. T. M., 1996. "Origin of high kurtosis in viscous sublayer". *Physics of Fluids,* ***8***, pp. 1938–1942.
[39] Xu, C., 2010. "Multi-scale analysis of subgrid stress and energy dissipation in turbulent channel flow". *Acta Mechanica Sinica,* ***26***(1), pp. 81–90.
[40] Cui, G., Chen, Y., Zhang, Z., Xu, C., Shao, L., and Bertoglio, J., 2000. "Transportation of passive scalar in inhomogeneous turbulence". *Acta Mechanica Sinica,* ***16***(1), pp. 21–28.
[41] G, L., W, B., L, S., and et al., 2007. "Decay of scalar variance in isotropic turbulence in a bounded domain". *Journal of turbulence,* ***8***(1), pp. 1–11.
[42] Fang, L., Cui, G. X., Xu, C. X., and Zhang, Z. S., 2005. "Multi-scale analysis of energy transfer in scalar turbulence". *Chinese Physics Letters,* ***22***(11), pp. 2877–2880.
[43] Yeung, P., 1994. "Spectral transfer of self-similar passive scalar fields in isotropic turbulence". *Physics of Fluids,* ***7***, p. 2245.
[44] Fang, L., Shao, L., Bertoglio, J., Cui, G., Xu, C., and Zhang, Z., 2009. "An improved velocity increment model based on kolmogorov equation of filtered velocity". *Physics of Fluids,* ***21***(6), p. 065108.
[45] Spalart, P. R., Jou, W. H., Strelets, M., and Allmaras, S. R., 1997. "Comments on the feasibility of les for wings, and on a hybrid rans". *Advances in DNS/LES*, p. 137.
[46] Lévêque, E., Toschi, F., Shao, L., and Bertoglio, J., 2007. "Shear-improved Smagorinsky model for large-eddy simulation of wall-bounded turbulent flows". *Journal of Fluid Mechanics,* ***570***, pp. 491–502.
[47] L.Shao, Zhang, Z., Cui, G., and Xu, C. X., 2005. "Subgrid modeling of anisotropic rotating homogeneous turbulence". *Physics of Fluids,* ***17***(11).